Journal of Hydrology 540 (2016) 340–354

Contents lists available at ScienceDirect

Journal of Hydrology

journal homepage: www.elsevier.com/locate/jhydrol

Integration of Volterra model with artificial neural networks for rainfall-runoff simulation in forested catchment of northern Iran

Mahsa H. Kashani [a,*], Mohammad Ali Ghorbani [a], Yagob Dinpashoh [a], Sedaghat Shahmorad [b]

[a] Department of Water Engineering, University of Tabriz, Tabriz, Iran
[b] Faculty of Mathematical Sciences, University of Tabriz, Tabriz, Iran

ARTICLE INFO

Article history:
Received 20 February 2016
Received in revised form 4 June 2016
Accepted 13 June 2016
Available online 16 June 2016
This manuscript was handled by Andras Bardossy, Editor-in-Chief, with the assistance of Purna Chandra Nayak, Associate Editor

Keywords:
Artificial neural network
Volterra model
Rainfall-runoff process
Simulation
Northern Iran

ABSTRACT

Rainfall-runoff simulation is an important task in water resources management. In this study, an integrated Volterra model with artificial neural networks (IVANN) was presented to simulate the rainfall-runoff process. The proposed integrated model includes the semi-distributed forms of the Volterra and ANN models which can explore spatial variation in rainfall-runoff process without requiring physical characteristic parameters of the catchments, while taking advantage of the potential of Volterra and ANNs models in nonlinear mapping. The IVANN model was developed using hourly rainfall and runoff data pertaining to thirteen storms to study short-term responses of a forest catchment in northern Iran; and its performance was compared with that of semi-distributed integrated ANN (IANN) model and lumped Volterra model. The Volterra model was applied as a nonlinear model (second-order Volterra (SOV) model) and solved using the ordinary least square (OLS) method. The models performance were evaluated and compared using five performance criteria namely coefficient of efficiency, root mean square error, error of total volume, relative error of peak discharge and error of time for peak to arrive. Results showed that the IVANN model performs well than the other semi-distributed and lumped models to simulate the rainfall-runoff process. Comparing to the integrated models, the lumped SOV model has lower precision to simulate the rainfall-runoff process.

1. Introduction

A model of the rainfall–runoff (R-R) relationship is an essential component in the evaluation of water resources projects. This relationship is known to be highly nonlinear and complex due to large spatial and temporal variability of catchment characteristics, temporal and spatial patterns of precipitation and the number of input variables involved in the model. Based on the degree of representation of the involved physical processes, R-R models classified as black-box models, conceptual models and physically-based distributed models (Napiorkowski, 1986).

Conceptual models or physically-based models simulate R-R process mainly based on the meteorological and physiographical characteristics of catchment. It is usually difficult for engineers to apply these models as they have insufficient data or knowledge on hydrologic system processes (Chang et al., 2007). To resolve these problems, most hydrologists have adopted the black box models, which often avoid addressing the mentioned problems. Hence, Volterra integral series (VIS) and then artificial intelligence (AI) techniques as black box models have been introduced (Sajikumar and Thandaveswara, 1999; Khatibi et al., 2011). The Volterra model is a general mathematical model for a non-linear black-box system that produces a single output from a serial input (Muftuoglu, 1991). The Volterra models can fit any complex dynamic systems, without necessity to assume model structure. Volterra filters have been successfully used in modeling numerous physical applications, especially in signal processing and system identification. According to Singh (1988), Amorocho and Orlob were probably the first investigators to have exploited the VIS by introducing the functional series models (FSM) for the analysis of hydrologic systems. A detailed discussion on FSM, as applied to hydrologic system, is available in Amorocho (1973). Diskin and Boneh (1972) described the nonlinear relationship between excess rainfall and direct surface runoff by a Volterra series. Papazafiriou (1976) simulated R-R process using open time-invariant linear and second-order nonlinear Volterra models with memory. Napiorkowski (1986) used a model in the form of a second-order approximation of a cascade of nonlinear reservoirs to model flow in open channels and surface runoff systems. Such a model was equivalent to the first two terms of the Volterra series. Labat et al. (1999) applied Volterra first order and second order convolution

* Corresponding author.
E-mail address: mahsakashani2003@yahoo.com (M. H. Kashani).

http://dx.doi.org/10.1016/j.jhydrol.2016.06.028
0022-1694/

and a new nonlinear threshold model based on the frequency distribution of inter-annual mean daily runoff to two karstic watersheds in the French Pyrenees Mountains, using long sequences of rainfall and spring outflow data at two different sampling rates (daily and semi-hourly). Sajikumar and Thandaveswara (1999) applied an artificial neural network (ANN) paradigm, known as the temporal back propagation neural network (TBP-NN), as a monthly R-R model. The performance of this model in a "scarce data" scenario was compared with Volterra type FSM. Chou (2007) proposed a wavelet-based efficient modeling of nonlinear R-R processes and its application to flood forecasting in a river basin. A discrete wavelet transform was used first to decompose and compress the Volterra kernels and then Kalman filters were utilized to estimate online compressed wavelet coefficients of the Volterra kernels, and thus model the time-varying nonlinear R-R processes. Maheswaran and Khosa (2012) combined wavelet decomposition with Volterra models to forecast one month ahead of streamflow and compared it to wavelet-based linear models, linear regression models and other nonlinear approaches such as the coupled wavelets-ANN-based models. Kamruzzaman et al. (2013) compared the Volterra model and other time series models for streamflow that use lagged rainfall as an exogenous variable, with models that use a small subset of discrete wavelet coefficients of lagged rainfall with cross product and quadratic terms of the wavelet coefficients in three catchments in the Murray Darling Basin.

AI techniques are black-box and data-driven bottom-up modeling approaches without any prior assumptions about the model structure. These models are intelligent in the sense that they use a proportion of the data points from the time series to identify their inherent structure and use the remaining data points for validation of predictions. ANNs are AI techniques that have gained significant attention in recent years and play an important role in hydrology nowadays due to their ability to provide better solutions for modeling complex systems that are poorly described or understood. An ANN learns about its environment through an iterative procedure known as training that adjusts the parameters (weights) of the network. An early work by Halff et al. (1993) involved a three-layer feed-forward ANN using rainfall hyetographs as input and hydrograph as output. Zhu and Fujitha (1994) then compared the performance of fuzzy reasoning in R-R modeling and a feed-forward ANN model in predicting a 3-h lead runoff. Subsequently, a number of studies have employed ANN for R-R modeling (e.g. Smith and Eli, 1995; Abrahart and See, 2000; De Vos and Rientjes, 2005; Talei et al., 2010; Sarkar and Kumar, 2012; Kashani et al., 2014).

In contrast to the application of ANNs, the application of functional series requires the kernel to be evaluated and estimated by means of techniques such as the Brandstetter–Amorocho methods (Amorocho and Brandstetter, 1971) and the least-squares method. However, the functional series can be calibrated adaptively, although the extra effort in doing so may not be worth it in terms of results. Moreover, the application of ANN in R-R modeling does not require any a priori assumption regarding the processes involved. The advantages of an ANN compared to conventional models, are discussed in detail by French et al. (1992).

However, most of the Volterra and ANN models reported in literature have been applied as lumped models for R-R simulation and used a total rainfall value over the catchments in the input vectors (Napiórkowski and Strupczewski, 1979; Smith and Eli, 1995; Labat et al., 1999; Tayfur and Singh, 2006; Chou, 2007; Sarkar and Kumar, 2012; Kashani et al., 2014). Since the R-R process varies with spatial and temporal scales and affects the overall model performance, the lumped models cannot simulate it precisely. In some recent studies, the ANNs and conceptual models have been combined and applied as a semi-distributed integrated model to estimate the river flow with less error (Jeong and Kim, 2005; Ashu and Sanaga, 2006; Chen and Adams, 2006; Nilsson et al., 2006; Kamp and Savenijie, 2007; Corzo et al., 2009; Hou et al., 2011). The conceptual model of these combined models is usually for stream flow of every sub-catchment and the ANN model is for assembling the stream flow from each sub-catchment. However, these combining models have not avoided the requirement of parameters for conceptual model for every sub-catchment and have disadvantage of requirement of spatial variations parameters about physical characteristics of the catchments.

The innovation of this study is to expose a semi-distributed integrated model including two different black-box models i.e., the ANN and Volterra models to simulate the R-R process. The Volterra model will model the R-R process in each sub-catchment without requiring physical characteristic parameters of the sub-catchments and the ANN will assemble the stream flow from each sub-catchment. Since this proposed model is defined to simulate the R-R in each sub-catchment, so the model explores spatial variation in rainfall-runoff process as a semi-distributed model. Furthermore, both of the Volterra and ANN models are black-box models and they will not require any other catchment physical parameters (such as area and slope).

The rest of this article is organized as follows. The next section describes the structure of the Volterra model in a discrete time system after having been identified by the conventional matrix method. Then, description of the ANN is presented. A case study of application of the proposed method to a catchment in north of Iran is then presented. Finally, results are described and discussed, and conclusions are drawn.

2. Materials and methods

2.1. Volterra model

The Volterra series are an important representation of a nonlinear system. Given the input u and output y variables of the model, the Volterra kernels are identified by solving some linear equations (Chou, 2007). The discrete form of the Volterra model is written as:

$$y_k = \sum_{j=1}^{m_1} h(j)u_{k-j} + \sum_{i=1}^{m_2}\sum_{j=1}^{m_2} g(i,j)u_{k-i}u_{k-j} + \cdots + \varepsilon_k = y_{1k} + y_{2k} + \cdots + \varepsilon_k \quad (1)$$

where $h(j)$ and $g(i, j)$ indicate the first-order kernel and second-order kernel of the Volterra model, respectively, which act as the weighting coefficients on the past input to the system. The m_1 and m_2 are the length of data or memory in the linear and nonlinear parts of the Volterra model, respectively. The length of the inputs (u) of the model should be greater than $2m_1$ and $2m_2$ (Napiórkowski and Strupczewski, 1984). The y_{1k} and y_{2k} state the Volterra model output obtained at the linear and nonlinear parts of the Volterra model, respectively, and the ε_k represent the random noise (with zero mean) of the model output.

The major drawback of the Volterra model is the exponential growth of the model parameters with the memory and order of the model, which causes problems on identification of the model particularly when the system is strongly nonlinear (Goulart and Burt, 2012). Since, an infinite Volterra series is not possible to implement in a practical study, a truncated Volterra model is used. Lattermann (1991) corroborated the heuristic finding that including a second term to the linear hydrological model is useful for an accurately approximation, so the present study uses a second-order Volterra model for the R-R process. The second-order Volterra (SOV) model is defined as follows:

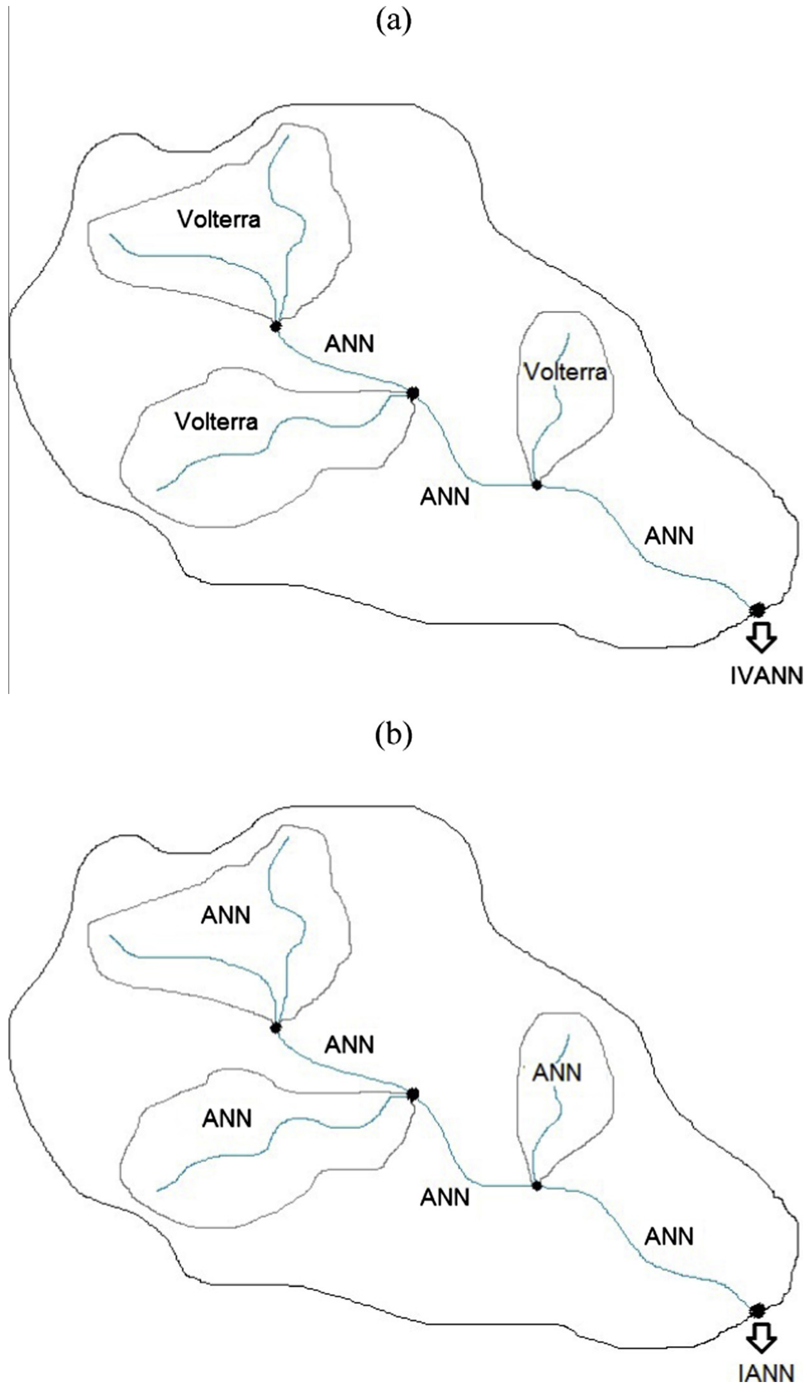

Fig. 1. Schematic diagram of applying the integrated models to an assumed catchment, (a) IVANN model, (b) IANN model.

$$y_k = \sum_{j=1}^{m_1} h(j)u_{k-j} + \sum_{i=1}^{m_2}\sum_{j=1}^{m_2} g(i,j)u_{k-i}u_{k-j} + \varepsilon_k \tag{2}$$

2.1.1. Identifying the SOV model

One of the major tasks in modeling of nonlinear systems using the Volterra model is to determine the Volterra kernels in time domain. In this study, the OLS method is applied to identify the nonlinear Volterra model because it is the most straightforward method for solving the Volterra model. Assume that discrete convolution structure of the system is as follows (Nikolaou and Mantha, 2000);

$$y_k = \sum_{j=1}^{m_1} h(j)u_{k-j} + \sum_{i=1}^{m_2}\sum_{j=1}^{m_2} g(i,j)u_{k-i}u_{k-j} + \varepsilon_k = \boldsymbol{u}_{1k}^T\boldsymbol{h} + \boldsymbol{u}_{2k}^T\boldsymbol{G}\boldsymbol{u}_{2k} + \varepsilon_k \tag{3}$$

where $\boldsymbol{h} = [h_1, h_2 \cdots h_{m_1}]^T$, $\boldsymbol{u}_{1k} = [u_{k-1}, u_{k-2} \cdots u_{k-m_1}]^T$, $\boldsymbol{u}_{2k} = [u_{k-1} \cdots u_{k-m_2}]^T$ and the symbol T stands for transposition. The coefficient matrix $\boldsymbol{G}$ of the kernel is assumed to be symmetric with no loss of generality. Therefore, only $M_2 = m_2(m_2+1)/2$ coefficients (of the m_2^2 second-order coefficients) are determined. The linear coefficients number is equal to $M_1 = m_1$. All elements in the lower-triangular part of matrix $\boldsymbol{G}$ are constructed the vector $vec_{lt}(G)$. Then y_{2k} can be stated as:

$$y_{2k} = \boldsymbol{u}_{2klt\Omega}^{T} \boldsymbol{g}_{lt} \tag{4}$$

where $\boldsymbol{u}_{2klt\Omega} = \Omega_{m_2}\, vec_{lt}(\boldsymbol{U}_{2k}), \boldsymbol{U}_{2k} = \boldsymbol{u}_{2k}\boldsymbol{u}_{2k}^{T}, \boldsymbol{g}_{lt} = vec_{lt}(\boldsymbol{G})$ and

$$\Omega_{m_2} = diag\left(\underbrace{1,2,2,\cdots 2}_{m_2\ elements}\ \underbrace{1,2,2,\cdots 2}_{m_2-1\ elements}\cdots\ \underbrace{1}_{1\ elements}\right)$$

Therefore, the Volterra model as Eq. (3) can be written in the standard linear regression form as:

$$y_k = \phi_k^T \theta + \varepsilon_k \tag{5}$$

where $\phi_k = \begin{bmatrix} \boldsymbol{u}_{1k} \\ \boldsymbol{u}_{2klt\Omega} \end{bmatrix}$ and $\theta = \begin{bmatrix} \boldsymbol{h} \\ \boldsymbol{g}_{lt} \end{bmatrix}$. Therefore, the ordinary least squares (OLS) method can be used to estimate the unknown parameter θ. The OLS method produces the least-squares error between the observed (y_k) and estimated ($\hat{y}_k$) outputs. The objective function, F, is defined as:

$$F = \sum_{k=1}^{N} (y_k - \hat{y}_k)^2 \tag{6}$$

The minimization of the objective function F leads to an estimator of the kernels:

$$\hat{\theta} = [\phi_k \phi_k^T]^{-1} [\phi_k y_k] \tag{7}$$

2.2. Artificial neural network (ANN)

ANNs are parallel information processing systems consisting of a set of neurons or nodes arranged in layers and when weighted inputs are used, these nodes provide suitable conversion functions. Any layer consists of pre-designated neurons and each neural network includes one or more of these interconnected layers. Further information on ANNs can be found in Haykin (1999).

The type of ANN used in this study is a multi-layer feed-forward perceptron (MLP) trained with the use of back propagation learning algorithm. The MLP network consists of (i) input layer, I, (ii) hidden layer, H, and (iii) output layer, O. The operation of this network is such that the input layer accepts the data and the intermediate layer processes them and finally the output layer displays the outputs of the model. During the modeling stage, coefficients related to present errors in nodes are corrected through comparing the model outputs with recorded input data. Connection weights are first initialized randomly by assigning a small positive or negative random value through the following procedure:

1. Input–output patterns are selected randomly using the training data presented.
2. Actual network outputs are calculated for the current input after application to the activation function.
3. Performance measure is selected, e.g. Mean Square Error (MSE), and the values are calculated.
4. Connection weights are adjusted to minimize the MSE.
5. Steps (2)–(4) are repeated for each pair of input–output vector in the training data, until no significant change in the MSE is detected in the system.

The final connection weights are kept fixed at the completion of training and new input patterns are presented to the network to produce the corresponding output consistent with the internal representation of the input/output mapping.

In this study, the Levenberg-Marquardt (LM) algorithm is used for training the MLP networks (De Vos and Rientjes, 2005). The LM algorithm is often the fastest back propagation algorithm, and has been highly recommended as a first-choice supervised algorithm, although it does require more memory than other algorithms (Adeloye and Munari, 2006). Further information on the back propagation learning algorithms can also be found in Haykin (1999).

2.3. Integrated Volterra and ANN model (IVANN)

The integrated form of the Volterra and ANN models (IVANN) contains two parts. The first part is the Volterra (SOV) model applied for R-R simulation in each sub-catchments of the catchment; and the second part is the ANN model used for flow routing between the outlet of sub-catchments and outlet of the catchment (Fig. 1a). The proposed IVANN model has advantages of the semi-distributed models considering the spatial variation of the rainfall in the catchment by modeling the R-R process separately in each sub-catchment. Moreover, the integrated model takes advantage of the high potential of Volterra and ANN models as suitable models in nonlinear mapping and functional relationship establishment.

In this study, since the Navrood River catchment has one hydrometric station (Kholyan) at the center of the catchment, so it can have just one sub-catchment (consisting of some tributaries) and the Volterra model will simulate the R-R over the upstream sub-catchment and the ANN will route the flow from the outlet of the sub-catchment to outlet of the Navrood catchment. Note that the proposed IVANN model may not completely explore spatial variation in the R-R process over the Navrood catchment; however, it differs from the lumped model and performs similar to a semi-distributed model. Since, there is no other forested catchment in Iran having enough hydrometric stations inside the catchment; the authors selected the Navrood catchment as an internal case study with one hydrometric station inside the area. According to the hydrological processes in the Navrood catchment, tributaries are mainly fed by rainfall, sub-surface flows and snowmelt, respectively. Since there was not enough information and data about sub-surface flow, pipe flow and interflow, which generate the dominant runoff in the forested catchments; the rainfall-runoff process was simulated based on the surface runoff generated from the effective rainfall and having enough data at the hydrometric stations. More information about how to evaluate the dominate runoff generation mechanism and interpret the hydrographs observed at smaller intervals can be found in Bonell, 1993; Bonell et al., 1990, 2010; Krishnaswamy et al., 2012, 2013. However, Harun et al. (2002) applied ANN and HEC-HMS models for prediction of daily runoff just using the rainfall as inputs of the models in the forested Sungai Lui catchment with higher annual rainfall and runoff rates than the Navrood River catchment.

Snowmelt is determined by some meteorological factors such as temperature, and wind speed. Since, the Volterra model gets only one kind of input variable, so, input variables used for this model are the delayed and current rainfall values. The inputs of the ANN in the second part of the IVANN model include delayed and current flow data estimated at outlet of upstream sub-catchment (the Kholyan station) for flow routing in downstream.

2.4. Integrated ANNs model (IANN)

Similar to the IVANN model, the integrated form of the ANN models (IANN) contains two parts. However, the first part is the ANN model applied for R-R simulation in each sub-catchments of the catchment; but the second part is again the ANN model used for flow routing between the outlet of the sub-catchments and outlet of the catchment (Fig. 1b). The proposed IANN model has also advantages of the semi-distributed models and high ability of the ANN in nonlinear mapping.

In this study, the ANN model will simulate the R-R over the upstream sub-catchment and then the ANN will route the flow from the outlet of the sub-catchment to outlet of the Navrood catchment. An important problem in the ANN modeling is the choice of input variables. In order to simulate the rainfall-runoff process; one can use other hydrological variables such as evapotranspiration and depression storage values. However, since the aim of the study is to evaluate the role of rainfall in runoff generation, we used just the rainfall data as the input variables of the ANN. Furthermore, Since the Volterra model gets only one input variable, in order to compare performance of the IVANN with IANN model logically, the ANN input variables were taken as the same as the Volterra model i.e., the delayed and current rainfall values. However, we can say that the effect of other factors on R-R simulation has been considered indirectly. For example, the effect of infiltration or soil moisture has been considered indirectly for R-R modeling. The infiltration and soil moisture affect the effective rainfall rates; and if the infiltration rate decreases or soil moisture increases the effective rainfall values will increase. Similarly, the evaporation can also affect the direct surface runoff values; if the evaporation rates increase the runoff volume will decrease.

Similar to the IVANN, the inputs of ANN in the second part of the IANN model are the delayed and current flow data estimated at outlet of sub-catchment for flow routing in downstream.

3. Case study and data sets

This study uses R-R data of the Navrood River catchment located at Gilan Province in the north of Iran (Fig. 2). The area of the catchment is about 274 km^2. The catchment is located between 48° 35′–48° 54′E and 37° 36′–27° 45′N. It is a forested catchment with humid climate. The mean annual precipitation is 852.7 mm, and the mean slope of the catchment is 31.16%. Due to the topography of this catchment, the stream flow path lines are almost steep and relatively large floods occur in the catchment, leading to environmental damages. The Navrood River includes several tributaries. Since one hydrometer station (the Kholyan) is there within the catchment, the catchment can be divided into one sub-catchment. From the Navrood River catchment, hourly flood data were collected from two hydrometer stations located at center and outlet of the catchment (the Kholyan and Kharjagil) and hourly rainfall data were collected from three rain gauging stations

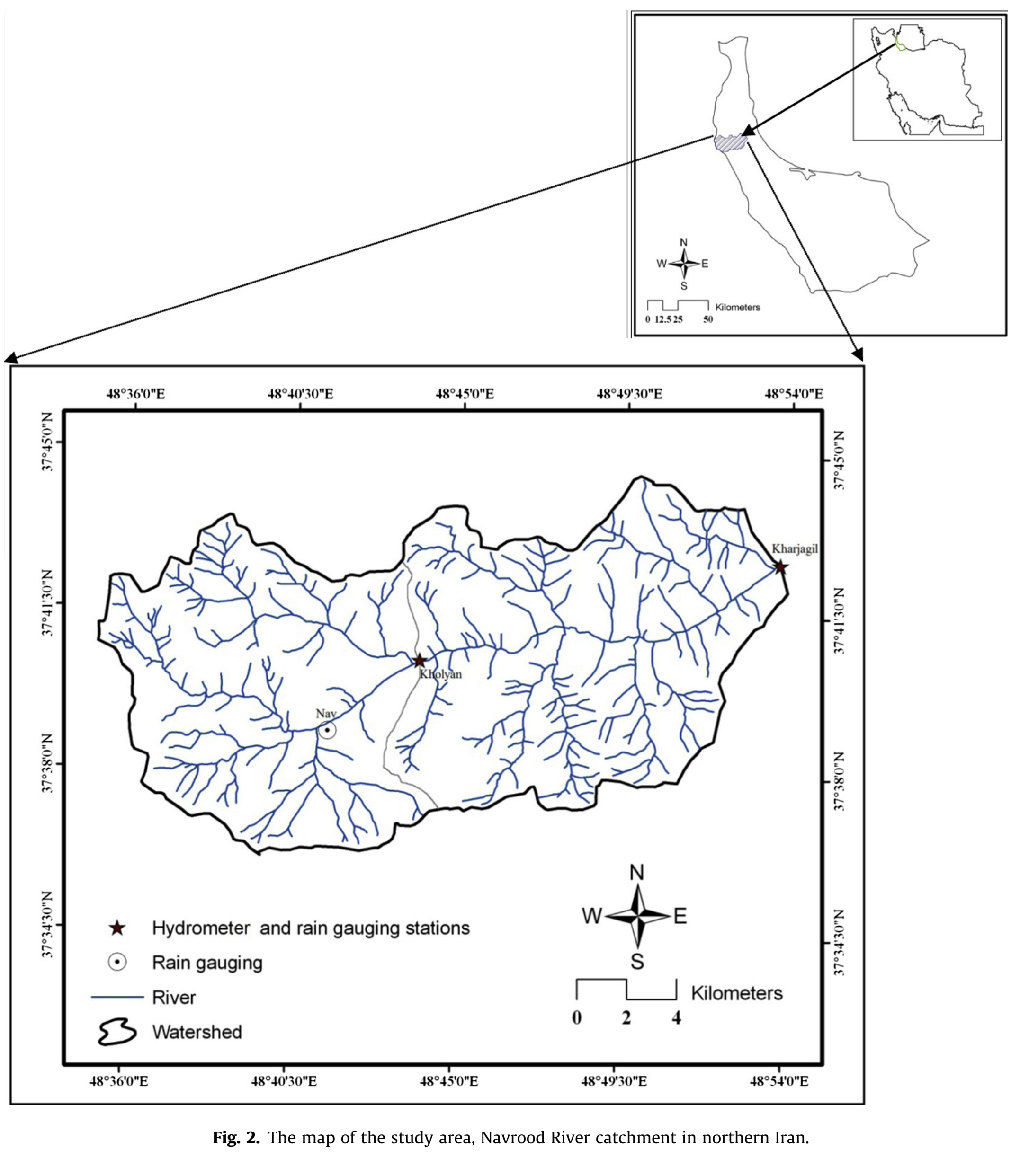

Fig. 2. The map of the study area, Navrood River catchment in northern Iran.

(the Nav, Kholyan and Kharjagil) within the catchment. Finally, thirteen simultaneous R–R storm events within the catchment and the sub-catchment in the period 1995–2005 were collected for this study. Although the catchment had also observed data from 2005 till 2014, they were not used to calibrate the models because the catchment has a reservoir, which was activated in this period on the Navrood River.

The areal averaged rainfall was computed using the Thiessen polygon method (Singh and Chowdhury, 1986) for the whole catchment and the sub-catchment. The effective rainfall rates were computed using the Φ index for each rainfall hyetograph of the events; and the direct runoff hydrographs were obtained by separating base flow from flood hydrographs using the constant-discharge method. Nine of the storm events (70%) were used for calibration of the Volterra and ANN models, while the other four (30%) were used for validation of the models. Details of the calibration and validation storm events are provided in Table 1.

4. Performance criteria for comparison of models

In order to quantitatively examine the performance of Volterra models, the one-hour ahead predictions were evaluated based on the following five performance criteria:

(1) Coefficient of efficiency, CE:

$$\mathrm{CE} = 1 - \frac{\sum_{i=1}^{n}(Q_i - \hat{Q}_i)^2}{\sum_{i=1}^{n}(Q_i - \bar{Q})^2} \tag{8}$$

where $\hat{Q}_i$ (m^3/s) and Q_i (m^3/s) represent the discharge of the simulated and observed hydrographs at the time i, $\bar{Q}$ (m^3/s) denotes the average observed discharge at the time i and n is the data points number. The closer the CE is to one, the better the fit.

(2) Root Mean Square Error (RMSE):

$$\mathrm{RMSE} = \sqrt{\frac{\sum_{i=1}^{n}\left(Q_i - \hat{Q}_i\right)^2}{n}} \tag{9}$$

(3) The relative error of total volume (EV) (Chou, 2007):

$$\mathrm{EV}\ (\%) = \frac{\sum_{i=1}^{n}(\hat{Q}_i - Q_i)}{\sum_{i=1}^{n}Q_i} \times 100\% \tag{10}$$

(4) The relative error of peak discharge ($\mathrm{EQ_p}$ (%)):

$$EQ_p(\%) = \frac{\hat{Q}_p - Q_p}{Q_p} \times 100\% \tag{11}$$

where $\hat{Q}_p$ (m^3/s) and Q_p (m^3/s) represent the peak discharge of the simulated and observed hydrographs.

(5) The error of the time-to-peak ($\mathrm{ET_p}$):

$$\mathrm{ET}_p = \hat{T}_p - T_p \tag{12}$$

where $\hat{T}_p$ (hour) and T_p (hour) denote the time-to-peak for the simulated and observed hydrograph, respectively.

Table 1
Details of storm events used in this study.

Events	Year	Areal averaged rainfall (mm/hr)	Peak discharge (m^3/s)	Areal averaged rainfall (mm/hr)	Peak discharge (m^3/s)
Calibration storm events					
		Kholyan station		Kharjagil station	
1	1995	0.18	3.10	0.49	9.93
2	1995	0.4	13.88	1.00	44.40
3	1995	0.94	8.20	1.18	25.55
4	1996	0.35	6.66	1.14	28.93
5	1998	1.36	45.45	1.69	127.62
6	1999	0.49	7.01	1.79	18.5
7	1999	0.74	10.96	0.94	47.8
8	1999	0.93	3.14	1.06	13.7
9	2000	0.56	4.77	0.68	19.55
Validation storm events					
1	2001	0.56	4.44	2.66	21.04
2	2001	0.52	9.05	0.90	22.11
3	2003	0.71	16.30	2.26	41.50
4	2005	0.30	2.77	0.36	8.00

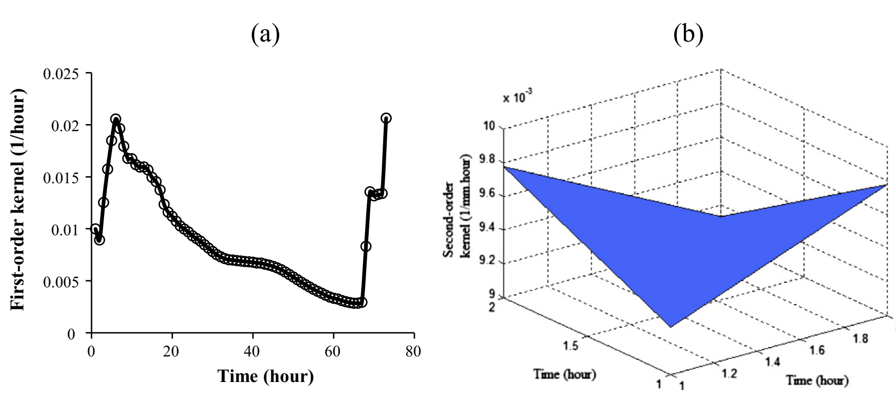

Fig. 3. The kernels of the lumped SOV model, (a) first-order kernel, (b) second-order kernel.

5. Results and discussion

5.1. Performance of the lumped SOV model

In this study, the SOV model cannot be calibrated using individual storm events because it includes many unknown parameters to be estimated. Therefore, nine storm events within the Navrood River catchment were connected in series and treated as a single storm event for the calibration. The time lag used for computations is 1 h, which is the same as the duration of the effective rainfall pulses. The numbers of parameters in the linear and nonlinear parts of the SOV model were chosen as 73 and 2 respectively, using trial and error to minimize the objective function (F) value. Since the dataset length (937 h) should be much greater than the memory length (73 and 2) for noise smoothing, the chosen parameters numbers seem to be correct. The first-order kernel of the SOV model calibrated using the OLS for the 9 events demonstrates that the OLS method does not yield a smooth kernel (Fig. 3a). This result is in agreement with the results obtained by Chou (2007) and Kashani et al. (2014), who found that conventional methods such as OLS for identifying the Volterra model are inefficient and

Table 2
Performance criteria of the lumped SOV model for the Navrood River catchment.

Events	RMSE (m^3/s)	EV (%)	CE	EQ_p (%)	ET_p (h)	*R*
		Calibration				
9 events in series	8.603	−25.396	0.639	−0.920	−3	0.823
		Validation				
Event 10	4.308	−24.119	0.442	14.667	−4	0.691
Event 11	3.669	−28.805	0.362	6.435	−1	0.867
Event 12	11.483	−44.037	0.072	−42.739	−5	0.551
Event 13	1.121	−31.110	0.554	−60.238	1	0.826
Average	5.145	32.018	0.357	31.020	2.75	0.734

Note: The columns for EV, EQ_p and ET_p all contain negative values, and these columns present the averages of the absolute values.

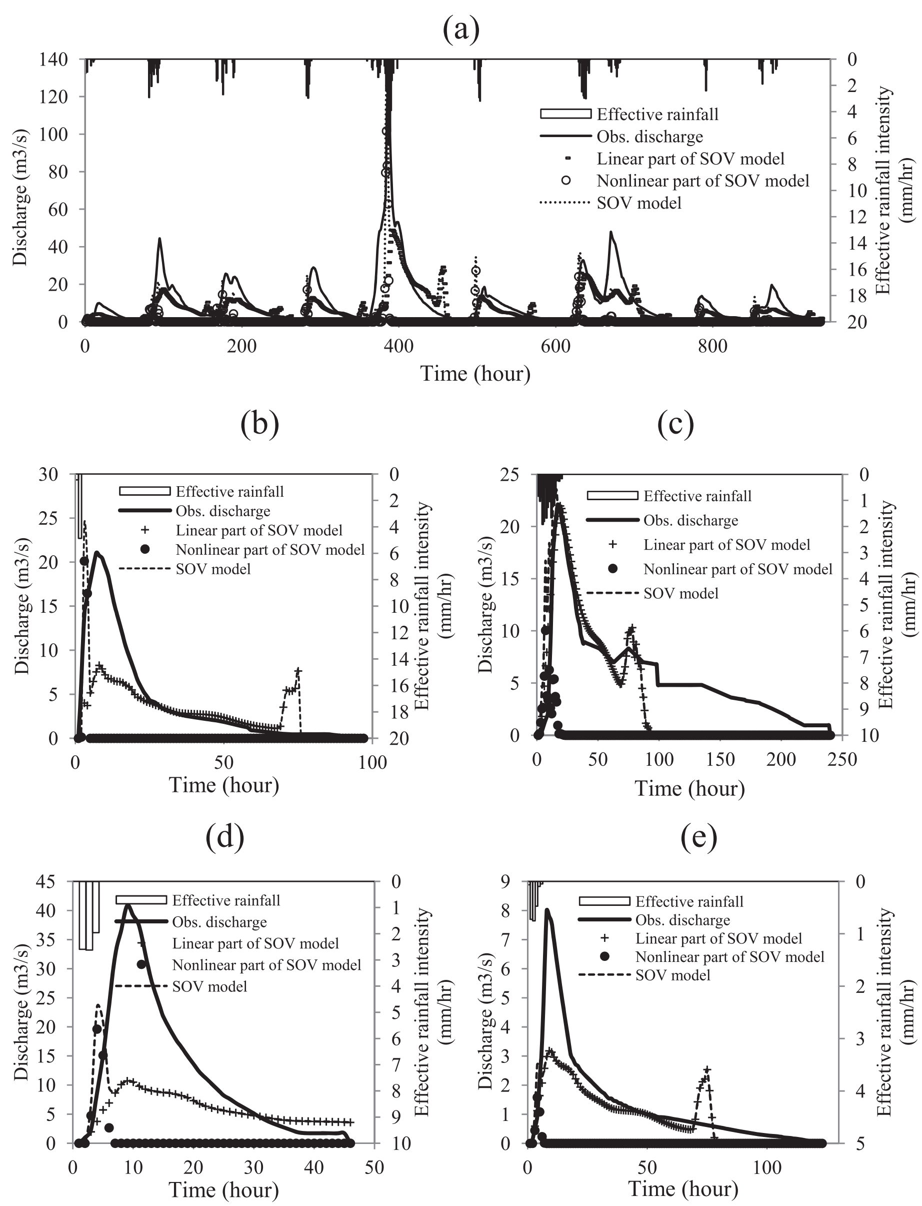

Fig. 4. The observed and estimated hydrographs of the SOV model at the calibration stage (a) and validation stage, (b) Event No. 10, (c) Event No. 11, (d) Event No. 12 and (e) Event No. 13.

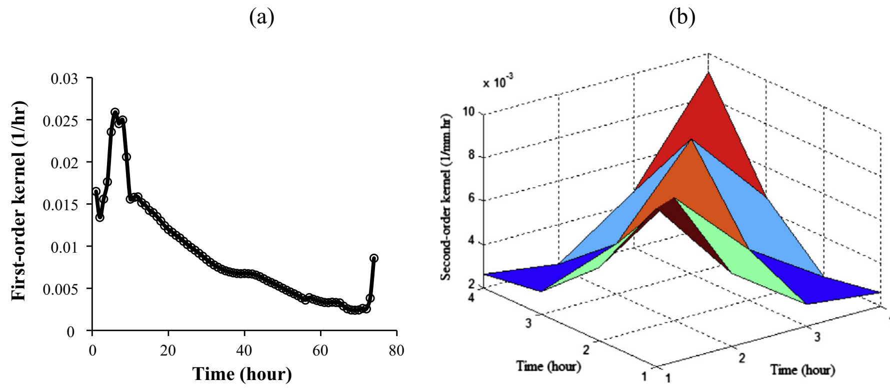

Fig. 5. The kernels of the IVANN model, (a) first-order kernel, (b) second-order kernel.

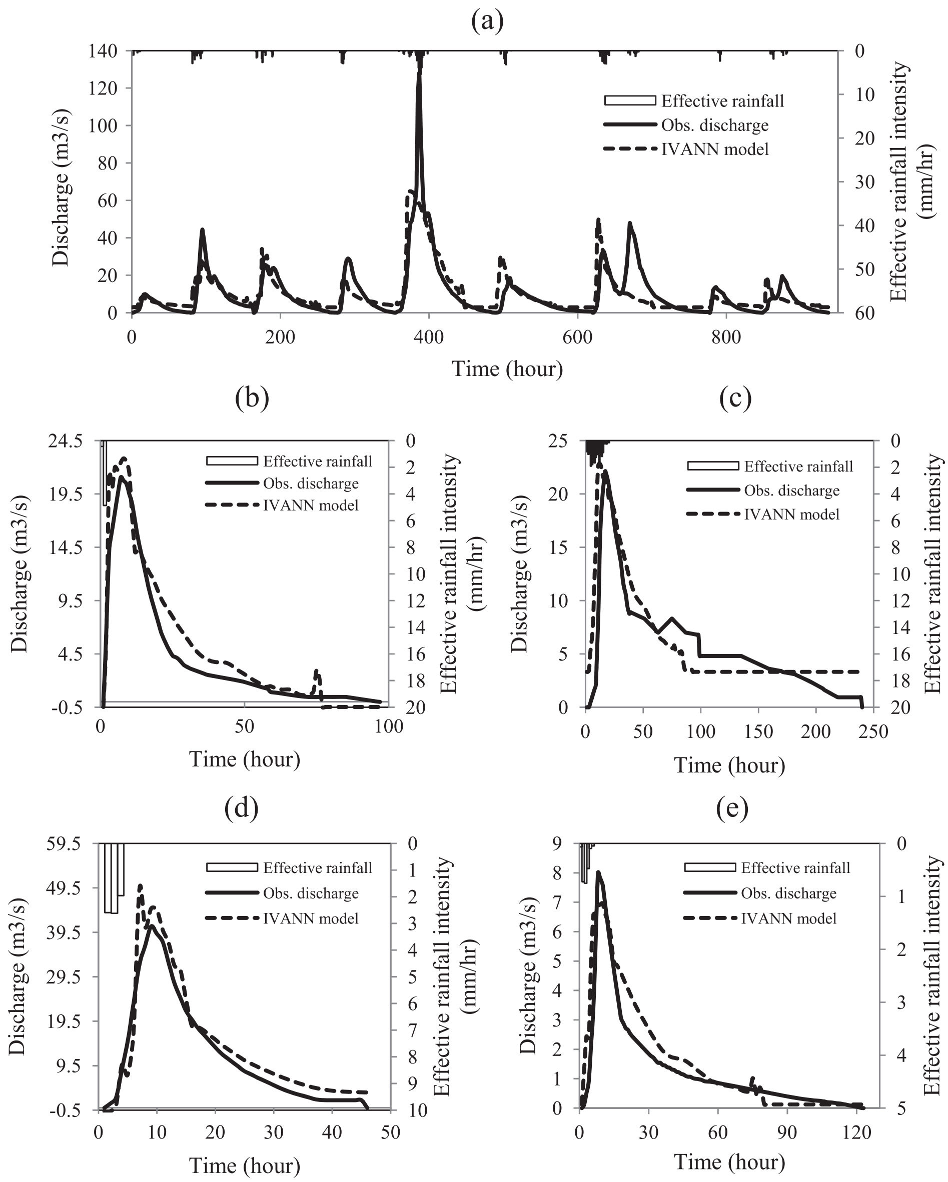

Fig. 6. The observed and estimated hydrographs of the IVANN model at the calibration stage (a) and validation stage; (b) Event No. 10, (c) Event No. 11, (d) Event No. 12 and (e) Event No. 13.

Table 3
Performance criteria of the IVANN model for the Navrood River catchment.

Events	RMSE (m^3/s)	EV (%)	CE	EQ_p (%)	ET_p (h)	R
			Calibration			
9 events in series	8.566	0	0.642	−49.190	−13	0.801
			Validation			
Event 10	1.812	21.468	0.901	8.486	1	0.974
Event 11	2.703	6.864	0.654	3.354	−5	0.850
Event 12	3.903	17.785	0.946	20.547	−2	0.972
Event 13	0.142	−3.504	0.959	−13.007	2	0.943
Average	2.140	12.405	0.865	11.348	2.5	0.935

Note: The columns for EV, EQ_p and ET_p all contain negative values, and these columns present the averages of the absolute values.

inaccurate because many parameters (here, 76) must be estimated. The kernel shape is similar to a hydrograph. It is characterized by a rising limb, followed by a falling limb. However, an upward trend is seen at the end of the kernel. Such a trend had been seen at the end of the first-order kernel obtained by Chou (2007) for a SOV model with 168 parameters. Likewise, the first-order kernels obtained by Labat et al. (1999) using two different identification methods for the linear Volterra model also were characterized by an upward trend at the end of the kernel. However, they obtained smooth kernels by using the Mixener polynomial method. The second-order kernel is not completely smooth and consists of only two sharpnesses (Fig. 3b). The smoother the kernel is, the better the model performance will be.

The calibration results obtained from the SOV model for the 9 storm events show that the SOV model estimates, the time to peaks and the rising limbs of the hydrographs more or less precisely (Fig. 4a). The peak flows are satisfactorily estimated just for some events. However, the falling limbs of the hydrographs are somewhat oscillated because of the unsmooth shape of the first-order kernel. Since the ordinates of the first-order kernel are multiplied by the input vector and then the output of the linear part of the model and the total output of the model is generated, therefore, the any oscillations on the first-order kernel are

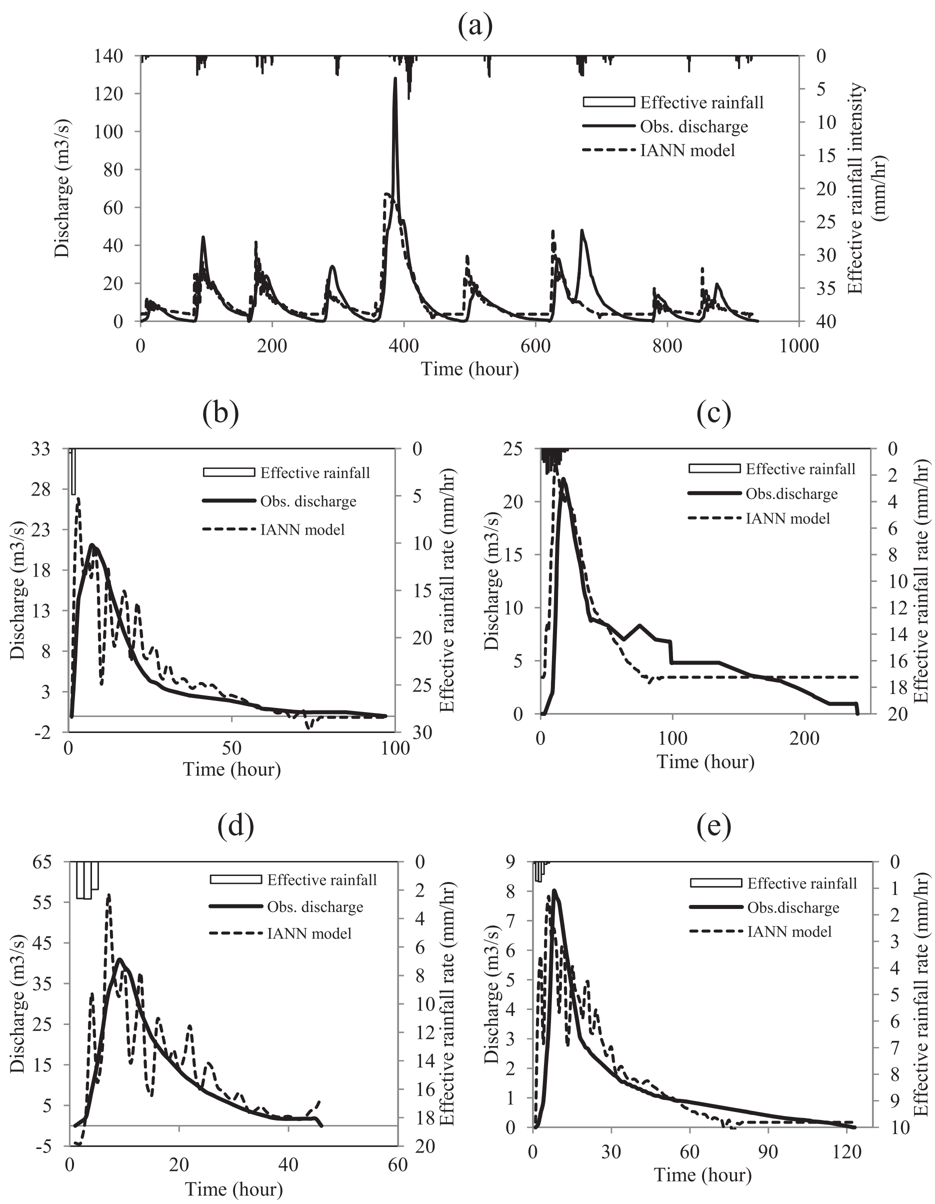

Fig. 7. The observed and estimated hydrographs of the IANN model at the calibration stage (a) and validation stage; (b) Event No. 10, (c) Event No. 11, (d) Event No. 12 and (e) Event No. 13.

Table 4
Performance criteria of the IANN model for the Navrood River catchment.

Events	RMSE (m^3/s)	EV (%)	CE	EQ_p (%)	ET_p (h)	*R*
			Calibration			
9 events in series	8.691	0	0.632	−47.455	−13	0.795
			Validation			
Event 10	3.219	10. 680	0.689	27.458	−5	0.859
Event 11	3.040	3.718	0.562	6.348	−6	0.803
Event 12	7.827	9.913	0.569	38.801	−2	0.806
Event 13	0.215	−8.234	0.908	−2.234	−2	0.812
Average	3.575	8.136	0.682	18.710	3.75	0.820

Note: The columns for EV, EQ_p and ET_p all contain negative values, and these columns present the averages of the absolute values.

transferred to the total output of the SOV model. The linear part of the model performs similarly; however, its estimated peak flows are somewhat low. The nonlinear part of the SOV model predicts the peak flows more accurately than the linear part; but, it estimates the falling limbs of the hydrographs with more error. Sum of the estimations of the linear and nonlinear parts of the SOV model generates the whole results for the SOV model. The performance criteria of the SOV model solved using the OLS method applied to 9 storm events connected in series reveals that the SOV model is fairly satisfactory (Table 2). The values of the all performance criteria are acceptable except the EV and RMSE which are almost high. At the validation stage, the SOV model overestimates the peak flow for the first two events (Fig. 4b and c) and underestimates them for the last two events (Fig. 4d and e). It estimates the time to peaks more successfully for the storm No. 11 and 13 (Fig. 4c and e) than the other events. The model predicts the rising limbs of the hydrographs precisely than the falling limbs. It shows a second peak flow at the end of the hydrograph for all the storms. This second peak can be due to the shape of the first-order kernel obtained at the calibration stage, which showed an upward trend at the end. The estimations of linear part of the SOV model are

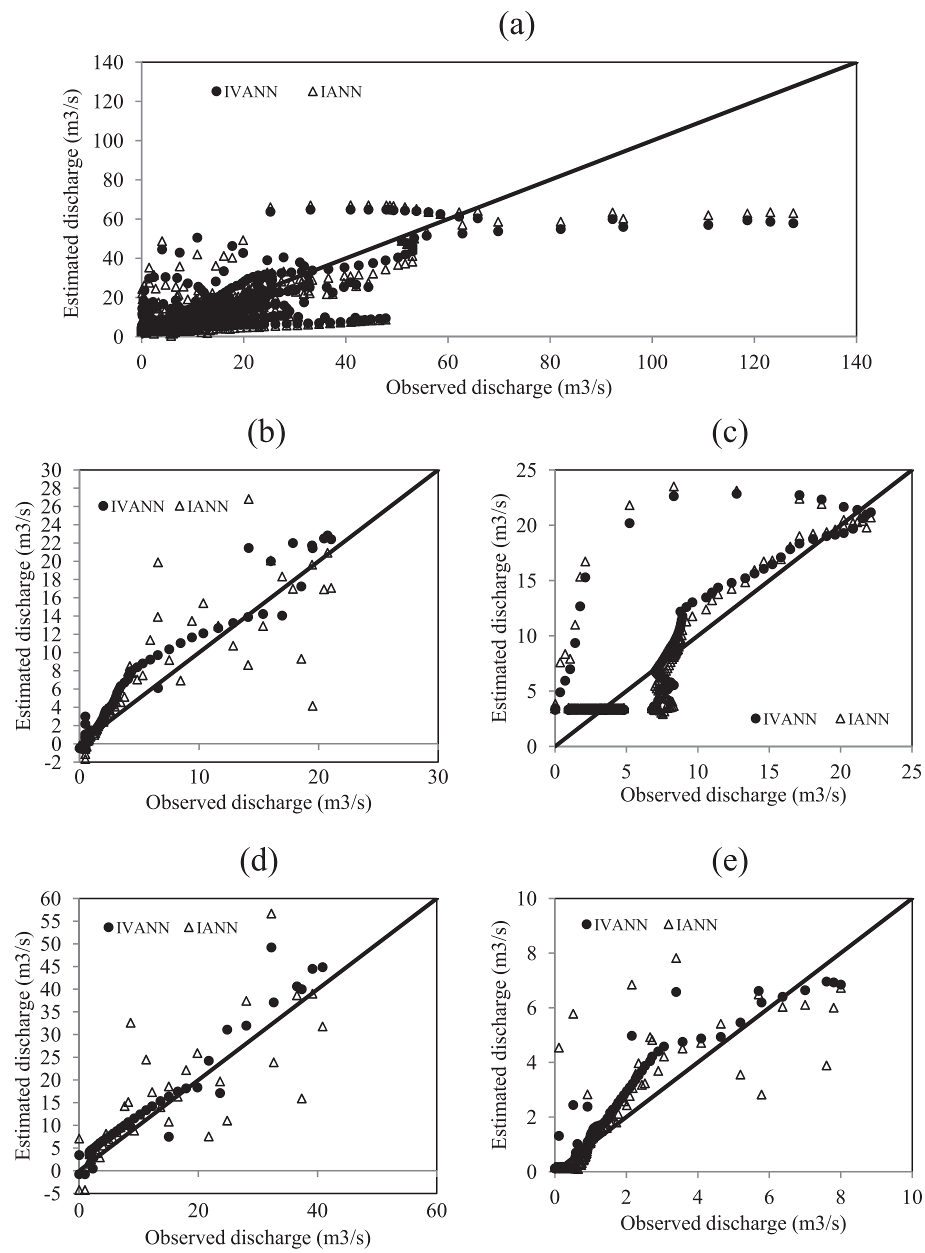

Fig. 8. Scatter plots of the observed versus estimated discharges of the IVANN and IANN models at the calibration stage (a) and validation stage, (b) Event No. 10, (c) Event No. 11, (d) Event No. 12 and (e) Event No. 13.

closer to the observed hydrographs and the SOV model, and their falling limbs coincide with each other for all the events; however, it underestimates the peak flows especially for events No. 10 and 12. The predicted peak flows and rising limbs of the nonlinear part of the model are closer to the observed hydrographs and SOV model for all the events. Note that the peak flows estimated by the linear part of the model is closer to the model rather than the nonlinear part for event No. 11 and 13. Generally, it seems that results of the linear part of the model have the most portions of the SOV results. However, the nonlinear part plays an important role on predicting the peak discharges and rising limbs of the hydrographs using the SOV model. According to Table 2, the average value of CE for the SOV is too low (0.357). Furthermore, the average value of the RMSE for the mentioned model is relatively high. According to the average value of the EV criterion, the SOV model does not perform satisfactorily and shows high total volume error. According to the EQ_p criterion value, the SOV model is not a very suitable model for protection and flood warning systems (with an average value of 31.020%). However, the ET_p value of the SOV model (with an average value of 2.75 h) indicates that it predicts the times of peak flows relatively precisely. Generally, the lumped SOV model demonstrated poor performance in the R–R simulation over the Navrood River catchment.

5.2. Performance of the IVANN model

5.2.1. R-R simulation in the sub-catchment using the Volterra model

In the upstream sub-catchment, the nine storm events were also connected in series and treated as a single storm event for calibration of the Volterra (SOV) model. The time lag used for computations is also 1 h, herein. The numbers of parameters in the linear and nonlinear parts of the SOV model were chosen as 74 and 4, respectively using trial and error. The first-order kernel of the SOV model obtained using the OLS method demonstrates that the OLS method does not again yield a smooth kernel (Fig. 5a). It has a small upward trend at the end of the kernel. The second-order kernel is not smooth and consists of one sharpness (Fig. 5b). However, these kernels are fairly smoother than the

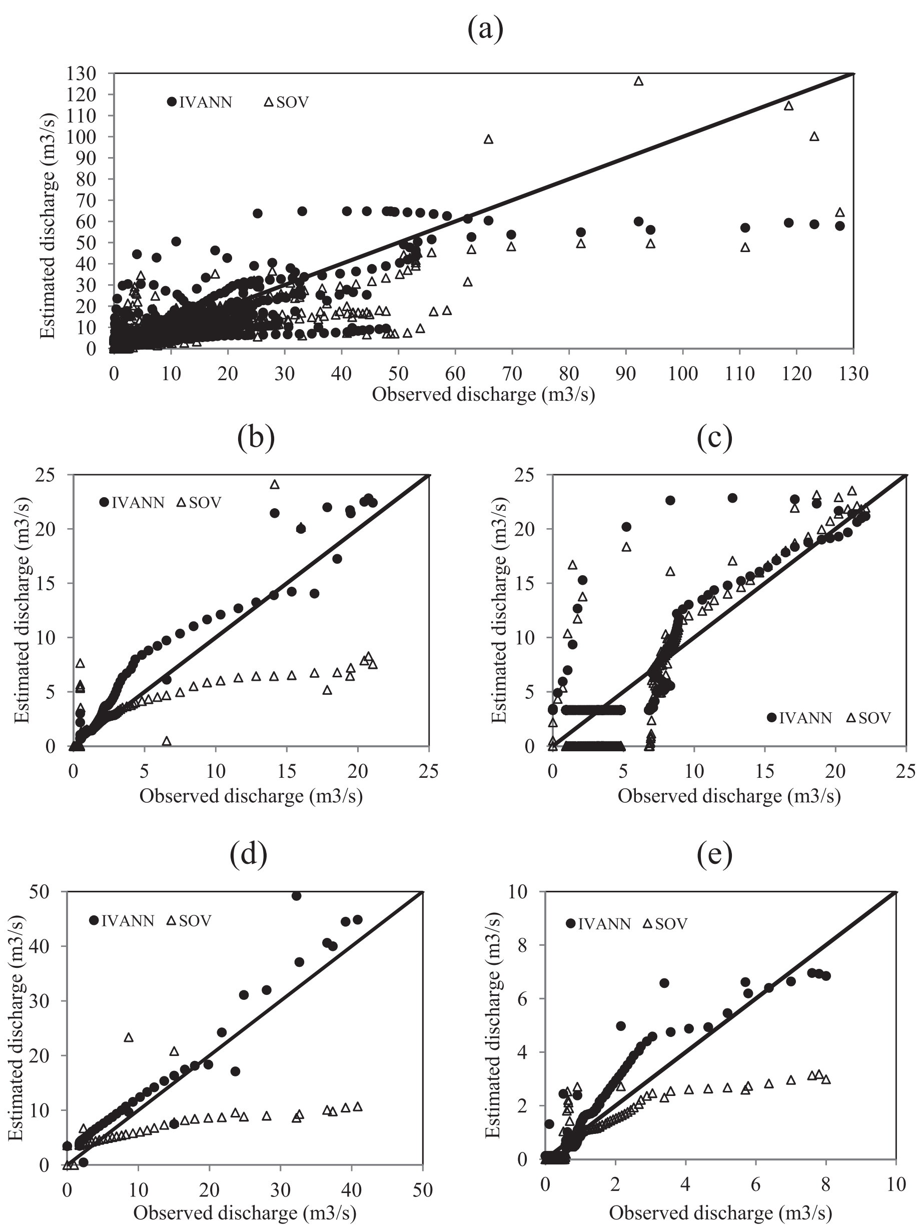

Fig. 9. Scatter plots of the observed versus estimated discharges of the IVANN and SOV models at the calibration stage (a) and validation stage, (b) Event No. 10, (c) Event No. 11, (d) Event No. 12 and (e) Event No. 13.

kernels obtained for the lumped SOV model. It means that this integrated (semi-distributed) model will perform well than the lumped one. This result was expectable because the semi-distributed models are more successful than the lumped models for R-R simulation. The calibration and validation hydrographs were calculated at the outlet of the sub-catchment using the SOV model and kernels obtained.

5.2.2. Flow routing using the ANN model

The ANN (MLP) model was implemented using the MATLAB software and the effective rainfall and direct surface runoff data were normalized using *mapstd* function to ensure that their mean is zero and standard deviation (σ) is one (Kashani et al., 2014):

$$X_n = \frac{X_i - \overline{X}}{\sigma} \tag{13}$$

where $\overline{X}$ represents the average observed data, and the subscripts i and n represent the ith data and normalized data, respectively. The ANN model was applied for flow routing between the outlet of the sub-catchment (Kholyan station) and catchment (Kharjagil station). The input variables for the MLP model were selected among different combinations of the delayed runoff estimated at the sub-catchment outlet using the SOV model. It was found that the best input variable is just the current runoff. The model output variable was the observed runoff data at the catchment outlet. The MLP model was trained using the levenberg-Marquardt (LM) training algorithm. The best fit model structure was determined for the MLP using the performance criteria and a trial-and-error method, which led to the identification of 1–1–1 structure (input layer with 1 neuron, hidden layer with 1 neuron using the tansigmoid function, and output layer with 1 neuron and using a linear transfer function in the output layer). The optimal structure obtained for the MLP has 4 parameters to be estimated. In this case, it seems that the size of the training data set (9 events or 937 sample data) is significant. However, this is not true for the Volterra model as a black-box model with 84 parameters. The calibration results obtained from the MLP (or IVANN) model for the 9 storm events, in which the output data of the MLP were denormalized for comparing the network performance with the observed data, indicate that the model estimates the time to peaks and the limbs of the hydrographs (except the last one) more or less precisely (Fig. 6a). The model overestimated three peak flows. However, it underestimated the main peak flow. According to the figure, it seems that all of the estimated hydrographs have some base flow, which is because of the ANN error in learning process. Table 2 shows the performance criteria of the model. It can be seen that, the values of all performance criteria except the EQ_p and ET_p are acceptable. The high value of the mentioned criteria is because of fairly poor performance of the model in estimating the 5th hydrograph having the highest peak flow. The results of the model for the other hydrographs are satisfactory. At the validation stage, the IVANN model predicts the peak flow, time to peak and the limbs of the hydrographs less or more accurately for all the events (Fig. 6b–e). According to Table 3, the IVANN model is more successful based on values of the all performance criteria. It can be concluded that the IVANN model has generally high potential in simulating the R–R process. This is due to the semi-distributed and non-linear nature of the model and also high ability of the SOV and MLP models.

5.3. Performance of the IANN model

5.3.1. R-R simulation in the sub-catchment using the ANN model

For applying the IANN model, first the MLP model was used to model the R-R process in the sub-catchment. It was found that the selected input variables for the SOV model (effective rainfall at time $(t-1), (t-2) \ldots$ and $(t-74)$) are the best inputs for the network. This means that the Volterra model has high ability in identifying the most effective input variables of the ANNs. Therefore, the input and output variables selected for the MLP model were the same as those for the SOV model in the sub-catchment. The MLP model was trained using the LM algorithm. The best fit structure of the MLP model was identified as 74–1–1 with tansigmoid and linear transfer functions for the hidden and output layers, respectively. The optimal structure obtained for the MLP has 77 parameters to be estimated. In this case, it seems that the size of the training data set (9 events or 937 sample data) is somewhat insignificant and this may cause the networks to show some errors in their estimations. This is also true for the SOV model as a black-box model with 74 parameters. In other words, one of the reasons for creating errors in the SOV performance was in signification of the dataset. However, the SOV model could treat this problem and thus caused the IVANN model to perform successfully. The validation hydrographs were predicted at the outlet of the sub-catchment using the MLP model.

5.3.2. Flow routing using the ANN model

After simulating the R-R over the sub-catchment, the river flow was routed from the outlet of the sub-catchment to outlet of the catchment using the MLP model. The input variables for the MLP model were selected among different combinations of the delayed runoff estimated at the sub-catchment outlet. The best input variable was the current runoff. The model output variable was again the runoff data at the catchment outlet. The MLP model was trained using the LM training algorithm. The best fit model structure was identified as 1–1–1 structure with the tansigmoid and linear transfer functions for the hidden and output layers, respectively. Here, the optimal structure obtained for the MLP has 4 parameters to be estimated. The calibration results obtained by the MLP model for the 9 storm events, in which the output data of the MLPs were denormalized for comparing the networks performance with the observed data, indicate that the model performance is not very satisfactory and estimates the rising limbs of the hydrographs more or less precisely (Fig. 7a). According to Table 4, the values of EQ_p and EQ_T are high. The model over-and under-estimated the peak flows of the hydrographs and this was caused the value of the EV to be zero. In other words, the zero value of the EV criterion cannot state good performance of the model. At the validation stage, the IANN model overestimates the peak flows for all the events except the last event (Fig. 7b –d). Both limbs of the predicted hydrographs (except event No. 11) are significantly oscillated. Note that the oscillations can also be seen on the limbs of the calibration hydrographs. Since the calibration hydrographs (9 events) are drawn compactly (Fig. 7a), their oscillations may not be seen obviously. The model shows errors in estimating the times to peaks for all the events. Moreover, the model estimates some notable negative discharge values for some components of the hydrographs (except No. 11). Generally, the model shows poor performance for the R-R simulation of the Navrood River catchment. Although Table 4 indicates relatively acceptable values for the performance criteria, the model performance is not satisfactory because of the oscillations on the hydrographs limbs. These oscillations have caused the RMSE and EV values not to increase a lot.

If the ANN model gets many input variables (here, 74 variables), the model will perform not accurately. Note that by using only 74 input variables, the model showed best performance which was not very satisfactory. This means that the model tried to learn just the smallest hydrograph (with short base time) for preventing to get more input variables. Modeling event-based R-R processes may be hard using the black-box models, because catchment characteristics may change during the events and so affect the R-R relationship and makes it complicate. In this case, the black-box models may not show high precise in their results while using just rainfall datasets. This may be why the ANN model was not more successful in simulating the process over the Navrood River sub-catchment. Here, it seems that the ANN model needs other hydrological data such as runoff as input variables to simulate the process with less error. Sarkar and Kumar (2012) also used rainfall and runoff data for modeling the event-based R-R process using the ANN. In this investigation, in order to compare the ANN model with the Volterra, their input variable was taken the same (rainfall).

5.4. Comparison of the performance of the integrated models

In order to compare performance of the two integrated models accurately, scatter plots of the models results were drawn (Fig. 8). According to the figure, it can be seen that the IVANN model performs better than the IANN model at the calibration stage. However, it seems that the IANN model is somewhat more able than the IVANN in predicting large flow values (flow more than 70 m^3/s). Note that the difference in their performance is not a lot at the calibration stage. Both of the models show more error in estimating large flows. This is due to the fact that number of hydrographs including large peak flows is small in the calibration period and this causes the models to show weakness in estimating such discharges. Fig. 8b–e shows that the performance of the IVANN model is obviously better than the IANN at the validation stage. However, for event No. 11 the difference is not significant.

Note that according to Fig. 8, the scatter plots between the observed and estimated discharges form loops. In Fig. 8c the loop is completely formed because the estimated hydrographs of the IANN and IVANN models are fairly wider than the observed hydrograph (see Figs. 6c and 7c). Since the IANN and IVANN models perform similarly for event 11, theirs loops are almost coincide with each other (Fig. 8c). In general, it can be concluded that although both of the models have advantages of semi-distributed models, the IVANN model is a more suitable model for R-R simulation. This means that the Volterra model has a high potential than the ANN in simulation of nonlinear R-R systems. The errors of the IVANN model are due to errors of the SOV and ANN models and also to the number of sub-catchments which is small (one) in this study. The semi-distributed models perform more accurately when the catchment consists of several sub-catchments. The error values of the SOV model depend on the identification method and also data quality and quantity. In other words, the ability of the Volterra model will be improved if a more precise method and high quality data are used for its identification and calibration. Here, performance of the ANN model depends on its input data quality i.e. the outputs of the SOV model which contain some errors.

5.5. Comparison of the performance of the integrated and lumped models

The validation results of the IVANN and IANN models are better than those of the calibration stage according to the statistical criteria. This is not true for the SOV model. This means that the IVANN and IANN models have been calibrated successfully because of the semi-distributed natures of the models. Furthermore, the characteristics of the validation events are similar to the calibration events. In other words, the selection of which events to use to calibrate and validate the models was successfully done; and data have been correctly divided into the calibration and validation parts (70% and 30%, respectively). Since, the IVANN model showed satisfactory results than the IANN, in this section performance of the IVANN model is compared with the lumped SOV model. Fig. 9 indicates scatter plots for these models. According to the figure, it is clear that the estimated discharges of the IVANN model are closer to the observed values. However, it seems that the lumped model is more successful in estimating large discharge value. This is due to the weakness of the ANN model in learning High flow values which are not significant at the calibration period. At the validation stage, it is obvious that the IVANN model performs more accurately than the SOV model for all events. This result was expected because the R-R process varies spatially and so the semi-distributed models are more suitable than the lumped models for simulating the process.

There are some common factors that lead to increase error in results of these models. One factor is applying the inefficient OLS method for identifying the SOV model. The OLS method is based on using high quality data. Since the rainfall and runoff data often includes some errors such as measuring errors, the OLS method is not a very efficient method for solving the R-R models. Moreover, when the model has many parameters to be estimated the OLS method will lose its ability for estimating the parameters precisely (Chou, 2007; Kashani et al., 2014). Moreover, the identification of kernels of the Volterra filters is a typical example of an ill-posed problem. It follows that one may find large errors of kernel estimates even if measurement errors are very small (Napiorkowski, 1986). However, it does not always lead to model over-fitting problem (Nikolaou and Vuthandam, 1998). The second factor is that the selected storm events had occurred in late summer and early autumn, in which the watershed is more likely not covered by snow. However, if the watershed was snow covered during that time, the direct runoff generated by excess rainfall may contain snow melt that can cause the models to not show precise results. In this case, it was better to consider the temperature variable as model input and investigate its effect on snow melts and models performance. The third factor is the method of separating base flow. In this study, the consistent discharge method was applied for this purpose, although this method is more common and popular method among the hydrologists, it is a very simple and thus inaccurate method. Using this method may cause to generate not very high quality runoff data and create errors in results of the models. The forth and similar factor is using the method for calculating the effective rainfall. Since in this method value of infiltration is assumed to be consistent during rainfall, it can cause to create errors in calculating the effective rainfall and then the models performance. The fifth factor is assuming that the R-R is time and spatial invariant. The rainfall and runoff values vary spatially over the catchment and even the sub-catchments. Furthermore, the rainfall and runoff values vary in time; and a model which can determine and update the obtained R-R relationship over a catchment will be a suitable model. In this study, the kernels obtained for the SOV models are consistent and not vary in time. In other words, the lumped SOV model and the semi-distributed IVANN model are time invariant models and so simulate the R-R process with some errors.

Note that the Volterra model presented better results than the ANN, while using the inefficient OLS method and just rainfall data as input variables. This means that the Volterra model has great potential than the ANN in R-R simulation especially when data are finite. Napiórkowski (1992) found that the Volterra model is suitable for loss-less systems (such as effective rainfall-direct runoff system). Moreover, Napiórkowski and Piotrowski (2005) concluded that the Volterra model shows better results than the ANN at the validation stage of R-R simulation. Here, the case study is a forested catchment in which rate of interception, infiltration, and transpiration may be high and considerable; therefore, the relationship between the rainfall and runoff may be more nonlinear and complicated. Therefore, nonlinear models such as IVANN can be more capable in simulating the R–R process of the catchment. This is in agreement with findings obtained by Kashani et al. (2014) that the linear first-order Volterra model is not a suitable model for the nonlinear R-R simulation over the Navrood River catchment.

6. Conclusions

The new approach of integration of Volterra model with artificial neural networks (IVANN model) for R-R process simulation have been developed and used in a forest catchment located in north of Iran. The calibration results showed that the OLS method used for identifying the Volterra model did not yield smooth kernels. The calibration and validation results indicated that the IVANN model showed great potential in R-R modeling comparing with the integrated ANN (IANN) and lumped Volterra (SOV) models. This proves high ability of the Volterra model than the ANN in R-R simulation. The IVANN model explored the spatial variation in R-R process; stream flow generated from the sub-catchment can be routed to generate stream flow at the outlet of catchment. The IVANN model retains advantages of the semi-distributed models considering the spatial variation of R-R process in the catchment, while taking advantage of the potential of Volterra and ANN as effective tools in nonlinear mapping. However, it need be pointed out that use of the integrated models is limited in some catchments where long-term hydrological data are lacking. This investigation constitutes a useful reference in which the nonlinear IVANN model is a very suitable model for simulating the R–R process. In order to improve the capability of the IVANN model, it is recommended to use more accurate methods such as the regularization and polynomial methods or intelligent methods such as genetic algorithms for identifying the model and use more high quality data for calibrating the model. Moreover, combining the model with Kalman filter is also recommended for updating models parameters and making the models time-variant. It is recommended to apply the proposed IVANN model for other catchments with different characteristics and climate conditions and compare the results. Likewise, investigations on applying the models for higher lead time forecasting need to be accomplished for better management of water resource systems. At the end, the authors suggest applying the proposed IVANN model at catchments where there are some sub-catchments with hydrometric stations at the outlets of them and evaluate its results and ability confidently.

Acknowledgments

We thank Dr. Nourani and Dr. Asadi for guiding and helping in collecting data. Thanks are also extended to the anonymous reviewers and editor (Dr. Andras Bardossy) for their constructive and useful comments that helped us improve the quality of the paper.

References

Abrahart, R.J., See, L., 2000. Comparing neural network and autoregressive moving average techniques for the provision of continuous river flow forecasts in two contrasting catchments. Hydrol. Proc. 14, 2157–2172.

Adeloye, A.J., Munari, A.D., 2006. Artificial neural network based generalized storage-yield-reliability models using the Levenberg–Marquardt algorithm. J. Hydrol. 362, 215–230.

Amorocho, J., 1973. Non-linear analysis of hydrologic systems. In: Chow, V.T. (Ed.), Advances in Hydroscience, vol. 9. Academic Press, New York, p. 203.

Amorocho, J., Brandstetter, A., 1971. Determination of nonlinear response functions in rainfall-runoff relations. Water Resour. Res. 7 (5), 1087–1101.

Ashu, J., Sanaga, S., 2006. Integrated approach to model decomposed flow hydrograph using artificial neural network and conceptual techniques. J. Hydrol. 317, 291–306.

Bonell, M., 1993. Progress in the understanding of runoff generation dynamics in forests. J. Hydrol. 150 (2–4), 217–275.

Bonell, M., Pearce, A.J., Stewart, M.K., 1990. The identification of runoff-production mechanisms using environmental isotopes in a tussock grassland catchment, eastern Otago, New Zealand. Hydrol. Process. 4 (1), 15–34.

Bonell, M., Purandara, B.K., Venkatesh, B., Krishnaswamy, J., Acharya, H.A.K., 2010. The impact of forest use and reforestation on soil hydraulic conductivity in the Western Ghats of India: implications for surface and sub-surface hydrology. J. Hydrol. 391 (1), 47–62.

Chen, J., Adams, B.J., 2006. Integration of artificial neural networks with conceptual models in rainfall–runoff modeling. J. Hydrol. 318, 232–249.

Chou, C.M., 2007. Efficient nonlinear modeling of rainfall-runoff process using wavelet compression. J. Hydrol. 332, 442–455.

Chang, F.J., Chang, L.C., Wang, Y.S., 2007. Enforced selforganizing map neural networks for river flood forecasting. Hydrol. Proc. 21, 741–749.

Corzo, G.A., Solomatine, D.P., Hidayat de Wit, M., Werner, M., Uhlenbrook, S., Price, R.K., 2009. Combining semi-distributed process-based and data-driven models in flow simulation: a case study of the Meuse river basin. Hydrol. Earth Syst. Sci. 13, 1619–1634.

De Vos, N.J., Rientjes, T.H.M., 2005. Constraints of artificial neural networks for rainfall–runoff modeling: trade-offs in hydrological state representation and model evaluation. Hydrol. Earth Syst. Sci. 9, 111–126.

Diskin, M.H., Boneh, A., 1972. Properties of the kernels for time invariant, initially relaxed, second order, surface runoff systems. J. Hydrol. 17 (1–2), 115–141.

French, M.N., Krajewski, W.F., Cuykendall, R.R., 1992. Rainfall forecasting in space and time using a neural network. J. Hydrol. 137, 1–31.

Goulart, J.H.M., Burt, P.M.S., 2012. Efficient kernel computation for Volterra filter structure evaluation. Sig. Proc. Lett. 19 (3), 135–138.

Halff, A.H., Halff, H.M., Azmoodeh, M., 1993. Predicting runoff from rainfall using neural networks. In: Kuo, C.Y. (Ed.), Engineering Hydrology, Proceedings of the Symposium Sponsored by the Hydraulics Division of ASCE, San Francisco, CA. ASCE, New York, pp. 760–765.

Harun, S., Ahmat Nor, N.I., Kassim, A.H.M., 2002. Artificial neural network model for rainfall-runoff relationship. J. Teknol. 37 (B), 1–12.

Haykin, S., 1999. Neural Networks: A Comprehensive Foundation, second ed. Prentice Hall, Upper Saddle River, New Jersey.

Huo, Z., Feng, S., Kang, S., Huang, G., Wang, F., Guo, P., 2011. Integrated neural networks for monthly river flow estimation in arid inland basin of Northwest China. J. Hydrol. 420–421, 159–170.

Jeong, D., Kim, Y., 2005. Rainfall–runoff models using artificial neural networks for ensemble streamflow prediction. Hydrol. Process. 19, 3819–3835.

Kamp, R.G., Savenijie, H.H.G., 2007. Hydrological model coupling with ANNs. Hydrol. Earth Syst. Sci. 11, 1869–1881.

Kamruzzaman, M., Metcalfe, A., Beecham, S., 2013. Wavelet based rainfall-stream flow models for the South-East Murray Darling Basin. J. Hydrol. http://dx.doi.org/10.1061/(ASCE)HE.1943-5584.0000894.

Kashani, M.H., Ghorbani, M.A., Dinpashoh, Y., Shahmorad, S., 2014. Comparison of Volterra model and artificial neural networks for rainfall–runoff simulation. Nat. Resour. Res. 23 (3), 341–354.

Khatibi, R., Ghorbani, M.A., Kashani, M.H., Kisi, O., 2011. Comparison of three artificial intelligence techniques for discharge routing. J. Hydrol. 403 (3–4), 201–212.

Krishnaswamy, J., Bonell, M., Venkatesh, B., Purandara, B.K., Lele, S., Kiran, M.C., 2012. The rain-runoff response of tropical humid forest ecosystems to use and reforestation in the Western Ghats of India. J. Hydrol. 472, 216–237.

Krishnaswamy, J., Bonell, M., Venkatesh, B., Purandara, B.K., Rakesh, K.N., 2013. The groundwater recharge response and hydrologic services of tropical humid forest ecosystems to use and reforestation: support for the "infiltration-evapotranspiration trade-off hypothesis". J. Hydrol. 498, 191–209.

Labat, D., Ababou, R., Mangin, A., 1999. Linear and nonlinear input/output models for karstic springflow and flood prediction at different time scales. Stoch. Env. Res. Risk Assess. 13, 337–364.

Lattermann, A., 1991. System-Theoretical Modelling in Surface Water Hydrology. Springer, Germany.

Maheswaran, R., Khosa, R., 2012. Wavelet-Volterra coupled model for monthly stream flow forecasting. J. Hydrol. 450–451, 320–335.

Muftuoglu, R.F., 1991. Monthly runoff generation by non-linear models. J. Hydrol. 125, 277–291.

Napiorkowski, J.J., 1986. Application of Volterra series to modeling of rainfall-runoff systems and flow in open channels. Hydrol. Sci. J. 31 (2), 187–203.

Napiórkowski, J.J., 1992. Comment on "Identification of a constrained nonlinear hydrological system described by Volterra functional series" by. J. Xia. Water Resour. Res. 28 (9), 2547–2549.

Napiórkowski, J.J., Piotrowski, A., 2005. Artificial neural networks as an alternative to the Volterra series in rainfall-runoff modeling. Acta Geophys. Pol. 53 (4), 459–472.

Napiórkowski, J.J., Strupczewski, W.G., 1979. The analytical determination of the kernels of the Volterra series describing, the cascade of nonlinear reservoirs. Hydrol. Sci. J. 6 (3–4), 121–142.

Napiórkowski, J.J., Strupczewski, W.G., 1984. Problems involved in identification of the kernels of Volterra series. Acta Geophys. Pol. XXXII (4), 375–391.

Nikolaou, M., Mantha, D., 2000. Efficient nonlinear modeling using wavelet compression. Progress in Systems and Control Theory, vol. 26, Boston.

Nikolaou, M., Vuthandam, P., 1998. FIR model identification: parsimony through kernel compression with wavelets. AIChE J. 44 (1), 141–150.

Nilsson, P., Uvo, C.B., Berndtsson, R., 2006. Monthly runoff simulation: comparing and combining conceptual and neural network models. J. Hydrol. 321, 344–363.

Papazafiriou, Z.G., 1976. Linear and nonlinear approaches for short-term runoff estimations in time invariant open hydrologic systems. J. Hydrol. 30, 63–80.

Sajikumar, N., Thandaveswara, B.S., 1999. A non-linear rainfall–runoff model using an artificial neural network. J. Hydrol. 216, 32–55.

Sarkar, A., Kumar, R., 2012. Artificial neural networks for event based rainfall-runoff modeling. J. Water Resour. Prot. 4, 891–897.

Singh, V.P., 1988. Hydrologic Systems: Rainfall-Runoff Modeling, vol. 1. Prentice Hall, Englewood Cliffs, New Jersey, 07632, p. 480.

Singh, V.P., Chowdhury, P.K., 1986. Comparing some methods of estimating mean areal rainfall. Water Resour. Bull. 22 (2), 275–282.

Smith, J., Eli, R.N., 1995. Neural-network models of rainfall-runoff process. J. Water Resour. Plann. Manage 121 (6), 499–508.

Talei, A., Chua, L.H.C., Quek, C., 2010. A novel application of a neuro-fuzzy computational technique in event-based rainfall-runoff modeling. Expert Syst. Appl. 37 (12), 7456–7468.

Tayfur, G., Singh, V.P., 2006. ANN and fuzzy logic models for simulating event-based rainfall-runoff. J. Hydraul. Eng. 132 (12), 1321–1330.

Zhu, M.L., Fujitha, M., 1994. Comparison between fuzzy reasoning and neural networks methods to forecast runoff discharge. J. Hydrosci. Hydraul. Eng. 12 (2), 131–141.